Self-compacting steel fibre reinforced concrete for precasted sandwich panels – experimental and numerical research

J. Barros, E. Pereira, A. Ribeiro & V. Cunha
Department of Civil Eng., School of Eng., University of Minho, Guimarães, Portugal.

J. Antunes
Civitest Company, Braga, Portugal.

ABSTRACT: In Portugal, steel fibres are the most used for concrete reinforcement, and flooring and tunnelling are the main applications of fibre reinforced concrete (FRC). In last years the prefabrication industry is showing more interest in collaborating in FRC research projects. The research carried out in consortium by University of Minho (UM) and two private companies for the development of self-compacting steel fibre reinforced concrete (SCSFRC) is an example of this new strategy. This research has the following main tasks: conceive a rational mix design method; evaluate the most relevant material properties and the structural behaviour of laminar elements; develop numerical tools. This paper intends to show the research strategy adopted in the SCSFRC project, since it is a typical example of the methodology followed by the UM research group, the most active in Portugal, in the FRC domain.

KEYWORDS: Self-compacting concrete, Post-cracking behaviour, Finite element analysis

1 INTRODUCTION

In Portugal, fibre reinforced concrete (FRC) is yet a material of relative reduced use in the Construction Industry. The fibre reinforcing system is practically restricted to steel fibres (SF), and flooring and tunnelling are the quasi-total applications of steel fibre reinforced concrete (SFRC). In recent years, polypropylene fibres are being added to SFRC in flooring applications, but without any technical or scientific support. Nevertheless, this practice has the benefit of restraining the micro-crack propagation in the concrete plastic shrinkage phase (Balaguru & Shah 1992).

In spite of the recognized economical and technical benefits of replacing conventional reinforcement, CR, (wire mesh and rebars) by SF in flooring applications, industrial pavements inconveniently reinforced with CR are still a significant percentage. Others structures of redundant supports and, consequently, of high stress redistribution capacity, have also high potential of being quasi-totally reinforced with discrete fibres, since internal forces of high magnitude only occur in well defined places (generally, in geometrical discontinuities of the structure). Tanks, wastewater stations, swimming pools, and underground infrastructures (Box-Culverts, pipelines, etc.) are examples of this type of structures but, in Portugal, the use of fibres as part of the reinforcing system is only adopted sporadically.

The precasting industry is specially appropriated for the development of innovative structural elements where fibre reinforcing system can be adopted with technical and economical benefits. However, panel elements to build façades are, practically, the unique application, where the reinforcing system is composed by glass fibres. This scenery is caused by the following main reasons: 1) lack of reliable design guidelines in the FRC domain; 2) inexistence of word-wide accepted standards for Lab and field FRC quality control; 3) deficient technical preparation on FRC domain of contractors, designers and fibre-sales-agents.

The majority of the Portuguese structural engineers support their design activity on officially approved Portuguese Standards. In recent years, some of them are using the Eurocode (CEB-FIP 1993). None of these documents, however, deals with the design of FRC. Therefore, the Portuguese structural designers are not confident on designing FRC structures. In fact, in spite of having passed more than 25 years since the first publication of ACI 544 about FRC, only recently a formulation for SFRC was developed under the framework of the Eurocode (ENV 1992-1-1 1992). This work was done by RILEM Technical Committee 162-TDF, that has resumed its technical and scientific effort in articles published in scientific journals (Vandewalle et al. 2002, 2003).

Since the majority of the structural engineers do not usually consults this type of publications, the knowledge included in these articles is only shared by researchers interested in FRC domain.

Attempting to overcome this reality, the University of Minho (UM) research group has the practice of promoting a Seminar at the end of a FRC research project, where the main relevant results are presented. With the same purpose, FRC is being taught in the UM post-graduate courses. The number of participants in these events is, however, not enough to change significantly the present scenario. A profound change will be only attained if FRC subjects start to be taught in the Civil Engineer Graduation and if a well-accepted FRC design formulation becomes to be available in the most used design model codes.

Furthermore, a well-accepted document about how to assure FRC quality control, not only in Lab conditions but also in the field, is essential for the confidence on the use of FRC. The RILEM TC 162-TDF did some work with this purpose (Vandewalle et al. 2002), but it is restricted to SFRC, and was published in journals and workshop's proceedings of reduced impact amongst contractors and designers. These agents need to know what FRC material properties should be characterized for design purposes and how they should be characterized. As this information is not yet available in the current design documents, the designers opt, normally, for one of the two following alternatives: refuse the option for FRC; accept a design suggested by a fibre-sales-agent. However, part of the fibre-sales-agents do not have the adequate technical and scientific preparation in FRC domain and it is usual practice to indicate a content of a given fibre, supported in a computational code that they do not understand the corresponding formulation, and without having the necessary data to perform a reliable design. This attitude contributes for the suspicion about the use of FRC.

In slabs on soil applications, the quality control of the applied FRC is practically inexistent. It is also usual to suppose a value for the soil reaction modulus that will be not checked anymore by soil-plate-tests. Therefore, cracking and excessive differential settlements are common in is type of applications.

In tunnelling, the practice of requiring plate tests is more common. However, apart reduced number of cases, the majority of the series of plate tests is only required to define the FRC mix composition. In Portugal, only EFNARC plate tests (EFNARC 1996) have been carried out, in spite of the recognized scatter on the energy absorption capacity that they provide. Lower scatter in the results can be obtained by the Round Determinate Panel (RDP) test, proposed by Bernard (Bernard 2002, ASTM-C-1550 2002) but, in Portugal, this test is yet not well known by the majority of the technicians working in tunnelling. More research and field work should be done in this subject, since RDP test appears to give more reliable information about the energy absorption capacity of FRC materials. Since in RDP test the support conditions remain constant during the test, as well as the crack pattern, the resulting force-deflection relationship reflects mainly the energy absorption capacity provided by fibre reinforcement mechanisms. Hundreds of EFNARC panel tests carried out in UM and Civitest Company have revealed that the panel support conditions and the developed crack pattern are mutually dependent, and both change during the test, which markedly influence the force-deflection relationship and, consequently, the evaluated energy absorption capacity.

As a result of the UM research effort, some Portuguese precasting companies are beginning to collaborate with UM research group. Self-compacting steel fibre reinforced concrete (SCSFRC) is a very promising composite material for the production of structural elements of complex geometry and/or composed by thin components. SCSFRC can also be used to reduce part of the conventional reinforcement in structural elements of high percentage of CR.

The present work deals with the experimental and numerical research carried out to conceive, produce and design sandwich SCSFRC panels for building façade applications. This research project involves Pregaia and Civitest Companies, and University of Minho. Like in other projects, the research carried out by UM research group involves a strategy for conceiving a rational FRC mix design method, an experimental program to characterize the material properties and the structural behaviour of representative prototypes, and numerical tools for the analysis and design.

2 APROACHES FOR THE FRC POST – CRACKING CHARACTERIZATION

The energy dissipated in concrete cracking is the most benefited property from the addition of fibres to concrete. To characterize toughness enhancement provided by fibre reinforcement mechanisms, ACI 544 proposed the concept of toughness index, $I_{(ACI)Old}$, which is the ratio between the energy dissipated by the FRC up to a

deflection of 1.9 mm, and the energy consumed up to crack initiation, δ_{cr}, see Figure 1, Golpalaratnam et al. (1991). This approach has, however, two deficiencies: the necessity of evaluating δ_{cr} with high accuracy, which is too difficult to assure, and the inexistence of a justification for the deflection limit value of 1.9 mm, under the framework of the limit state analysis required by design model codes. Attempting to overcome this drawback, ACI recommended the replacement of $I_{(ACI)Old}$ by the I_t index, see Figure 1. However, to evaluate I_t, the tests with the FRC and its corresponding plain concrete specimens should be carried out up to the total dissipation of the energy, which is difficult or even impossible to attain using flexural test set-ups. To evaluate the total energy dissipated in the fracture process of (FR)C materials, it should be carried out direct tensile tests in very high stiff, servo-controlled equipments (Barragán 2002, Noghabai 1998). However, this is a very time consuming test, since the energy is only totally dissipated at very large crack opening displacement (Noghabai 1998). Furthermore, behind a certain deflection/crack-opening level, the energy dissipated has no interest from the design point of view, which declines the design utility of the I_t index.

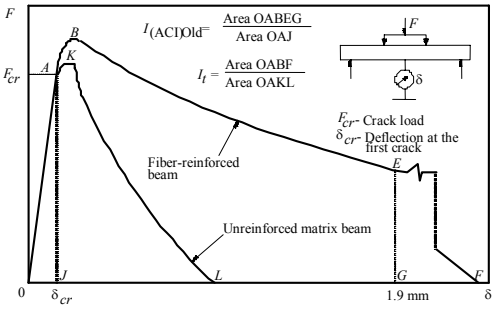

Figure 1. Toughness indexes proposed by ACI 544.

In 1990, ASTM C 1018 (1990) recommended the use of toughness indexes, I_N, schematically represented in Figure 2. These indexes represent the ratio between the energy dissipated up to given deflection limits and the energy exhausted up to crack initiation. An elastic-perfectly plastic material has values of 5, 10, 30, 50 and 100 for the I_5, I_{10}, I_{30}, I_{50} and I_{100}, respectively, see Figure 3. Like $I_{(ACI)Old}$ index, the toughness indexes are also susceptible to human judgment errors, since they require an accurate assessment of the deflection at crack initiation. Moreover, the deflection limits are not based on serviceability considerations.

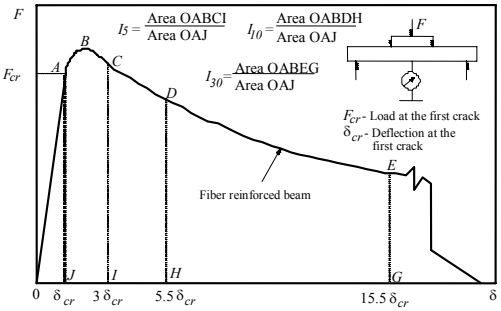

Figure 2. Toughness indexes proposed by ASTM C1018.

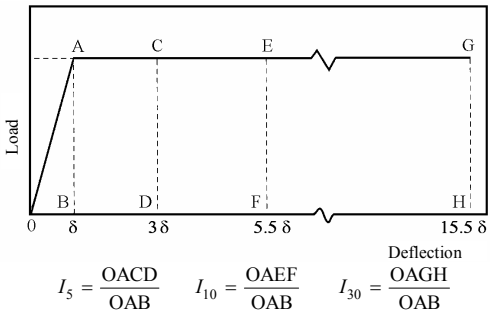

Figure 3. ASTM indexes for an elasto-perfectly plastic ideal material.

In 1984, the Japanese Society of Civil Engineers proposed the concept of flexural toughness factor, *FT*, represented in Figure 4 (JSCE 1984). The *FT* stress concept is calculated from the following expression:

$$FT = K \frac{L}{bh^2} \frac{D_f}{\delta_{150}} \quad (1)$$

where k = 1.0, since it is a four point bending test with equal distance amongst the point loads (150 mm), *b* and *h* are the width and the height of the beam cross section (150 mm), D_f is the energy dissipated up to the deflection $\delta_{150} = L/150$, where *L* is the beam span length (450 mm).

As Gopalaratnam et al. (1991), and Banthia & Trottier (1995a, b) have already pointed out, the *FT* concept of JSCE is dependent on specimen geometry, and the limit deflection δ_{150} is not based on considerations about limit state analysis.

Using a test set-up identical to JSCE, Banthia & Trottier (1995b) proposed the concept of post-crack strength, *PCS*. The main novelties of this concept are the exclusion of the energy up to peak load (energy not influenced by fibre reinforcement)

from the total energy up to given deflections, and the consideration of various deflection limits to cover distinct requirements on serviceability limit state analysis.

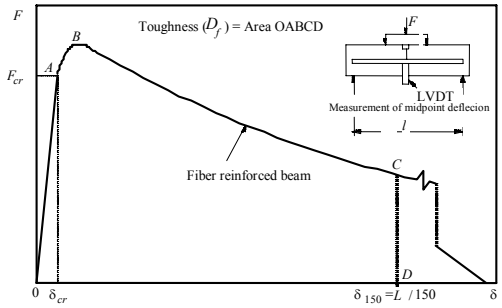

Figure 4. JSCE (1984) flexural toughness factor.

More recently, RILEM TC 162-TDF has proposed the concept of equivalent flexural tensile strength, f_{eq}, to characterize the post cracking behaviour of SFRC (Vandewalle et al. 2000a). This concept can be regarded as an improvement of the technique proposed by Banthia & Trottier (1995b). To decrease the scatter in the values generally reported when using four point unnotched beam tests (like JSCE and Banthia & Trottier test set up), RILEM TC 162-TDF proposed a three-point notched beam test. Since plain concrete shows a strain-softening phase, RILEM TC 162-TDF recommended a more precise procedure to exclude the parcel of energy due to matrix cracking from the total energy dissipated in the fracturing process of a SFRC material. The f_{eq} concept corresponds to *FT* of JSCE and *PCS* of Banthia & Trottier inasmuch as it is function of the energy dissipated up to a given deflection. However, it deviates from *FT* and *PCS*, since f_{eq} is presumed to take only into account the energy absorption capacity provided by fibre reinforcement mechanisms. Figures 5-6 represent the concept of f_{eq}. These parameters are related to the material energy absorption capacity up to a deflection of δ_2 and δ_3 and can be obtained from the following expressions:

$$f_{eq,2} = \frac{3}{2}\frac{D^f_{BZ,2}}{0.50}\frac{L}{bh^2_{sp}};\ f_{eq,3} = \frac{3}{2}\frac{D^f_{BZ,3}}{2.50}\frac{L}{bh^2_{sp}}\ [\text{N/mm}^2] \quad (2)$$

where $D^f_{BZ,2}$ and $D^f_{BZ,3}$ are the energy provided by fibre reinforcement mechanisms up to δ_2 and δ_3 deflection limits, respectively. These deflections are $\delta_2 = \delta_L + 0.65$ mm and $\delta_3 = \delta_L + 2.65$ mm, where δ_L is the deflection corresponding to the highest value of the load recorded up to a deflection or crack mouth opening displacements (CMOD) of 0.05 mm, F_L. In these expressions b=150 mm, L=500 mm, and h_{sp} (=125 mm) is the distance between the tip of the notch and the top of the cross section (notch deepness of 25 mm). Note that the parcel of the energy due to matrix cracking (D^b_{BZ}) is not considered in the f_{eq} evaluation.

More recently, RILEM TC 162-TDF proposed the replacement of f_{eq} for the concept of residual flexural tensile strength, f_R, which gives the stress for distinct deflections or CMOD (Vandewalle et al. 2002). Although this last concept has the advantage of being easier to evaluate, it is more susceptible to the irregularities of the force-deflection relationship registered in the tests. The concept of f_R is represented in Figures 5-6, and can be determined from the following expressions:

$$f_{R,1} = \frac{3}{2}\frac{F_{R,1}L}{bh^2_{sp}};\ f_{R,4} = \frac{3}{2}\frac{F_{R,4}L}{bh^2_{sp}}\ [\text{N/mm}^2] \quad (3)$$

where $F_{R,1}$ and $F_{R,4}$ are the forces at deflections of $\delta_{R,1}$ = 0.46 mm and $\delta_{R,4}$ = 3.0 mm, respectively.

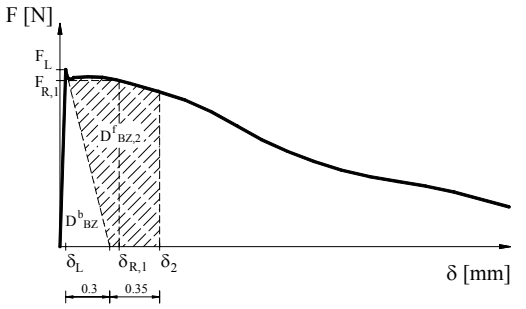

Figure 5. Evaluation of $f_{eq,2}$ and $f_{R,1}$ flexural tensile strength parameters according to RILEM TC 162-TDF (Vandewalle et al. 2000a, 2002).

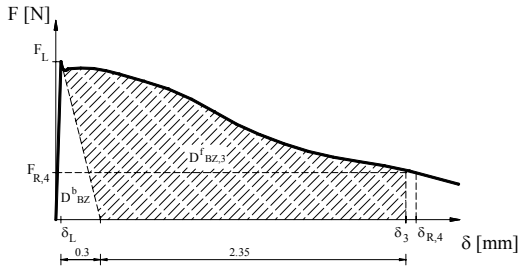

Figure 6. Evaluation of $f_{eq,3}$ and $f_{R,4}$ flexural tensile strength parameters according to RILEM TC 162-TDF (Vandewalle et al. 2000a, 2002).

According to RILEM TC 162-TDF (Vandewalle et al. 2000b, 2003), $f_{eq,2}$ or $f_{R,1}$ is used in the verifications of the serviceability limit states, while $f_{eq,3}$ or $f_{R,4}$ is applied in the ultimate limit state analysis, under the framework of the European pre-standard ENV 1992-1-12 (1992). The f_{eq} and f_R parameters were also used to define the stress-strain constitutive law proposed for modelling the SFRC post cracking behaviour (Vandewalle et al. 2000b, 2003).

3 SCSFRC COMPOSITION

The design of the SCSFRC composition was based on the three following steps: i) the proportions of the constituent materials of the binder paste are defined; ii) the proportions of each aggregate on the final solid skeleton are determined; iii) binder paste and solid skeleton are mixed in different proportions until self-compacting requirements in terms of spread ability, correct flow velocity, filling ability, blockage and segregation resistance are assured. This design strategy is described in detail elsewhere (Pereira et al. 2004).

The materials used in the SCSFRC were cement (C) CEM I 42.5R, limestone filler (LF), super-plasticizer (SP) of third generation based on polycarboxilates (Glenium® 77SCC), water (W), three types of aggregates (fine river sand, coarse river sand and crushed granite 5-12 mm) and DRAMIX® RC 80/60 BN steel fibres. This fibre has a length (l_f) of 60 mm, a diameter (d_f) of 0.75 mm, an aspect ratio (l_f/d_f) of 80 and a yield stress of 1100 MPa. Table 1 includes the content of each component per m^3 of the final SCSFRC.

Table 1. Mix proportions of the SCSFRC.

Cement	Water	SP	LF	Fiber
kg	kg	dm^3	kg	kg
364.3	93.7	6.9	312.2	30

Fine sand	Coarse sand	Coarse aggregate
kg	kg	kg
108.6	24.0	669.3

4 SCSFRC MECHANICAL PROPERTIES

The experimental program was composed by uniaxial compression tests with cylinders of 150 mm diameter and 300 mm height, and flexural tests with prismatic 600×150×150 mm^3 specimens. Both types of specimens were moulded without any external compaction energy. To assess the influence of the age of the SCSFRC on the compression and on the flexural behaviour, series of tests with specimens of 12 and 24 hours, and 3, 7 and 28 days were carried out.

4.1 *Compression*

The compression tests were carried out in a servo-controlled equipment of 3000 kN maximum load carrying capacity. Each test was controlled by the internal displacement transducer of this equipment, at a displacement rate of 5 µm/s. Three displacement transducers were positioned at 120 degrees around the specimen and registered the displacements between the load steel plates of the equipment. Taking the values recorded in these transducers, the displacement at the specimen axis was determined for each scan reading (Untiveros 2002), and the corresponding strain was obtained dividing this displacement by the measured specimen's height.

The stress-strain relationship for each testing age of the SCSFRC is represented in Figure 7. Each curve is the average of three specimens. Figure 8 and Figure 9 show the variation with the age of the average compressive strength, f_{cm}, and the average initial Young's Modulus, E_{cm}. From the analysis of these figures, the following observations can be pointed out: at 12 hours, the pre-established minimum limit of compressive strength of 20 MPa was already exceeded. At this age the f_{cm} is about 25 MPa while the E_{cm} is around 24 GPa. These properties increased with the SCSFRC age, reaching 62 MPa of f_{cm} and 36 GPa of E_{cm} at 28 days. At 24 hours, the f_{cm} and the E_{cm} was about 61% and 79% of the corresponding values at 28 days. In the first hours, E_{cm} has increased more pronouncedly than f_{cm}. Like ordinary concrete, the increase of the compressive strength resulted in a more fragile behaviour after peak load of the SCSFRC.

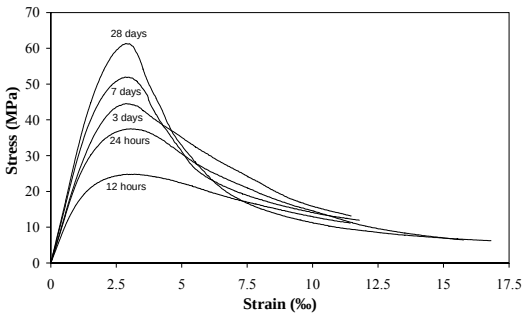

Figure 7. Stress-strain curves for SCSFRC cylinder specimens of distinct age at testing.

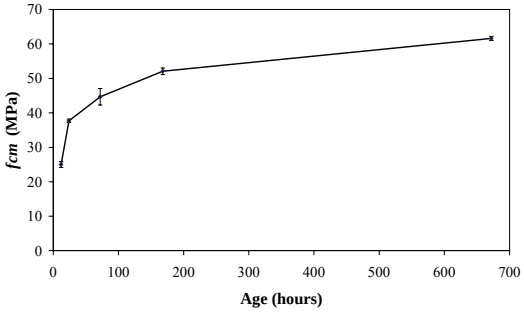

Figure 8. Influence of the SCSFRC age on its average compressive strength.

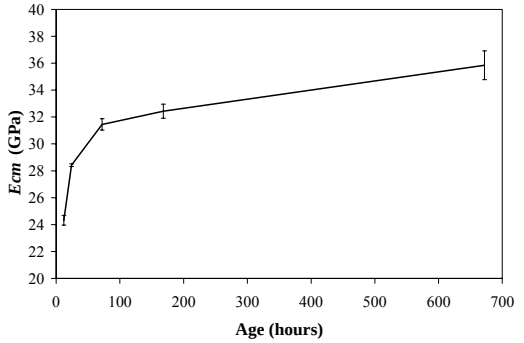

Figure 9. Influence of the SCSFRC age on its initial Young's modulus.

4.2 *Bending*

In the bending tests, the curing procedures, the position and dimensions of the notch sawn into the specimen, the loading and specimen support conditions, the characteristics for both the equipment and measuring devices, and the test procedures recommended by RILEM TC 162-TDF (Vandewalle et al. 2002) were adopted. The method for casting the beam specimens proposed by RILEM TC 162-TDF was adapted for SCSFRC since they were moulded without any external compaction energy.

The force-deflection curves, F-δ, obtained in the tested series are depicted in Figure 10. Each curve is the average of the F-δ relationship recorded in three specimens. The influence of the SCSFRC age in the force corresponding to the limit of proportionality, F_L, is graphically represented in Figure 11. This figure shows that F_L has increased with the SCSFRC age, but this increase became marginal after 7 days. Just after δ_L, a load decay has occurred with an amplitude that has increased with the SCSFRC age (see Figure 10), since a higher load should be sustained by the fibres bridging the specimen fracture surface. This load decay was followed by a hardening phase up to a deflection level that has decreased with the SCSFRC age. Except for specimens of 28 days, in the remaining the maximum load was larger than F_L. Apart series of 12 hours, in the remaining series the hardening phase was followed by a softening branch. The loss of residual strength in the softening branch was much more significant in series of specimens of 28 days. The larger amplitude of load decay just after δ_L in this series would have damaged the fibre-concrete bond and anchorage performances, leading to a decrease in the force necessary to pullout the fibres crossing the specimen fracture surface. In result of this, f_{eq} and f_R have only decreased between 7 and 28 days, see Figure 12. This decrease was more pronounced in the $f_{R,4}$ since this parameter is directly dependent on the shape of the force-deflection curve, and is evaluated for a deflection of 3.0 mm. As $f_{eq,2}$ and $f_{R,1}$ had similar variation with the age, this means that, for low values of deflection (δ_2 and $\delta_{R,1}$), the energy-based concept and the force-based concept provide identical results.

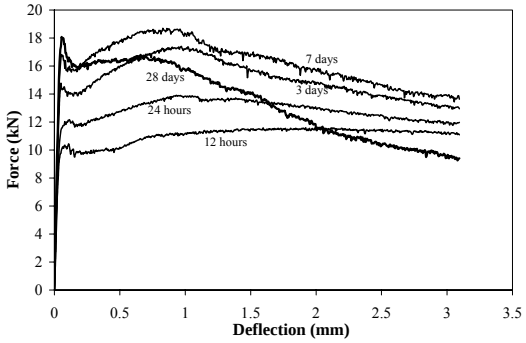

Figure 10. Force-deflection curves for SCSFRC beam specimens of distinct age at testing.

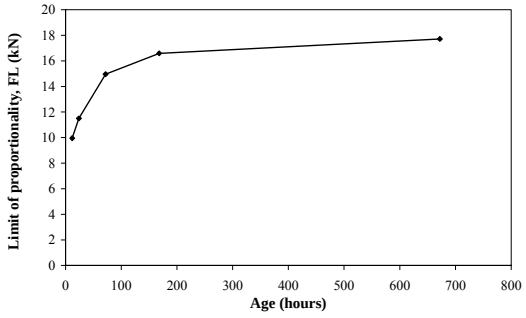

Figure 11. Influence of the SCSFRC age on the force at the limit of proportionality, F_L.

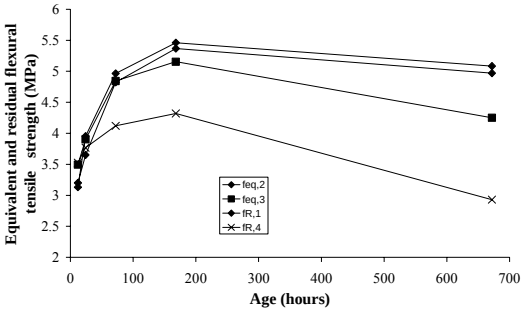

Figure 12. Influence of the SCSFRC age on the equivalent and residual tensile strength parameters.

5 INVERSE ANALYSIS TO ASSESS THE SCSFRC FRACTURE PARAMETERS

This section is dedicated to the assessment of the influence of SCSFRC age on the values of the fracture parameters of this material. Previous research has shown that the post-cracking behaviour of SFRC materials can be modelled by the trilinear stress-crack opening diagram, σ-*w*, represented in Figure 13 (Pereira et al. 2004, Sena et al. 2004a). To evaluate the aforementioned influence, an inverse analysis was carried out in order to obtain the dependence of the σ_i and w_i, that define the σ-*w* diagram, on the age of the SCSFRC. Knowing these dependencies, the influence of the SCSFRC age on its fracture energy (RILEM 50-FCM 1985) can be directly derived.

The inverse analysis was performed evaluating the values of the σ_i and w_i that best fit the experimental F-δ curves with the minimum error of the parameter,

$$err = \left| A_{F-\delta}^{\exp} - A_{F-\delta}^{num} \right| \Big/ A_{F-\delta}^{\exp} \qquad (4)$$

where $A_{F-\delta}^{\exp}$ and $A_{F-\delta}^{num}$ are the areas below the experimental and the numerical F-δ curves, respectively. For this purpose, a computational code named FEMIX was used, that has discrete and smeared crack models to simulate the crack initiation and crack propagation in cement based materials (Azevedo et al. 2003, Sena et al. 2004b). Since the RILEM TC 162-TDF flexural test brings up a localized fracture problem, a discrete crack model, described in detail elsewhere (Sena et al. 2004a), was used. Six-node 2D line interface finite elements were located in the specimen's symmetry axis to model the fracturing process. In the remaining parts of the specimen, eight-node Serendipity linear-elastic plane-stress elements were used. Gauss-Lobatto integration scheme (Schellekens 1990) with three integration points (IP) was used for the 2D line interface finite elements, while Gauss-Legendre integration scheme with 2×2 IP was used for the eight-node elements. To avoid undesired spurious oscillations of the stress field, a value of 1.0×10^4 N/mm^3 was assigned to the initial mode I stiffness for the interface element (Schellekens 1990). Since sliding between the fracture surfaces does not occur in this type of problem, the analysis is independent of the values assigned to the mode II stiffness of the interface element.

The adequacy of the numerical strategy adopted is shown in Figure 14, revealing that the proposed trilinear σ-*w* diagram is capable of predicting, with enough accuracy, the post-cracking behaviour of the tested specimens. The values for σ_i and w_i are included in Table 2 and correspond to the simulation of the average F-δ experimental curves.

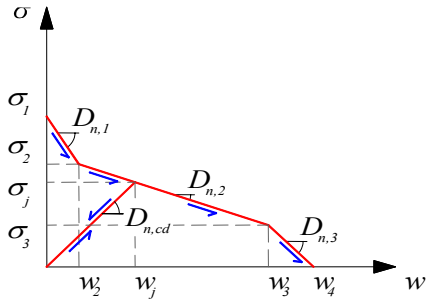

Figure 13. Adopted stress-crack opening diagram.

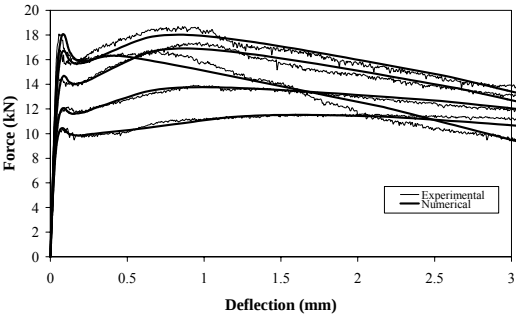

Figure 14. Experimental vs. numerical F-δ curves.

Table 2. Fracture parameters for SCSFRC of distinct ages.

Age	σ_1	w_1	σ_2/σ_1	w_3	σ_3/σ_1	w_4	G_f
days	MPa	mm		mm		mm	N/mm
0.5	1.52	0.06	0.7	1	0.85	9	6.37
1	1.80	0.06	0.7	0.5	0.88	8	6.62
3	2.25	0.06	0.68	0.5	0.88	5	5.31
7	2.60	0.06	0.65	0.5	0.80	5	5.64
28	2.92	0.06	0.58	0.25	0.62	4	3.90

As Figure 15 shows, σ_i increase up to 7 days. After this age, σ_1 continues to increase, σ_2 maintains practically constant, and σ_3 decreases. From Figure 16 it seems that the age has a tendency to reduce the values of the w_3 and w_4, while w_2 is not affected by the age of the specimen. This means that the slope of the first softening branch of the σ-w diagram, $D_{n,1}$, increases with the age. The second branch, $D_{n,2}$, reflects a "hardening process" of similar stiffness for the specimens of 3, 7 and 28 days, whose value is larger than those obtained in specimens of 12 and 24 hours, see Figure 17. Finally, all specimens had a third σ-w softening branch, of similar slope for the specimens of 12 and 24 hours, whose value is lower that those of specimens of 3, 7 and 28 days. The greater inclination of the softening branches and the smaller amplitude of the "hardening" branch of the σ-w diagram of the specimens of 28 days reflect the larger brittle character of the F-δ response registered in these specimens.

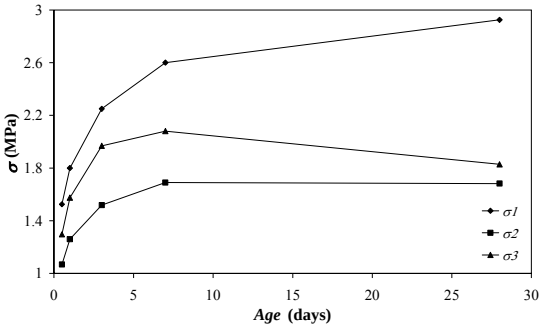

Figure 15. Influence of the SCSFRC age on the σ_i.

As indicated in section 2, TC 162-TDF recommended the use of $f_{R,4}$ to the ultimate limit state analysis for modelling the contribution of the fibre reinforcement. The $f_{R,4}$ is the stress for a deflection $\delta_{R,4}$ = 3.0 mm. Therefore, only the fracture energy dissipated up to this deflection, $G_{f,3mm}$, has interest from the design point of view. The influence of the SCSFRC age on the evolution of the $G_{f,3mm}$ is represented in Figure 18, from which it can be concluded that $G_{f,3mm}$ increases up to 7 days, followed by a significant decrease after this age. This means that the fibre reinforcing mechanisms were not sufficiently benefited by the increase of the matrix strength with the age in order to assure the tendency observed in the specimens tested up to 7 days. To avoid the decrease of the $G_{f,3mm}$ after 7 days, a higher content of fibres should be applied.

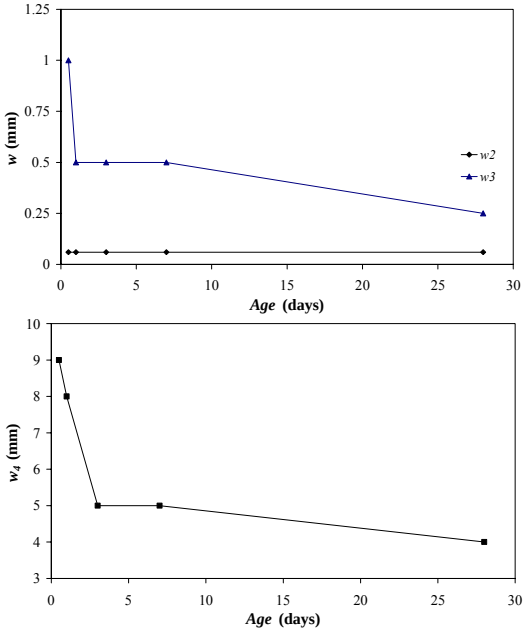

Figure 16. Influence of the SCSFRC age on the w_i.

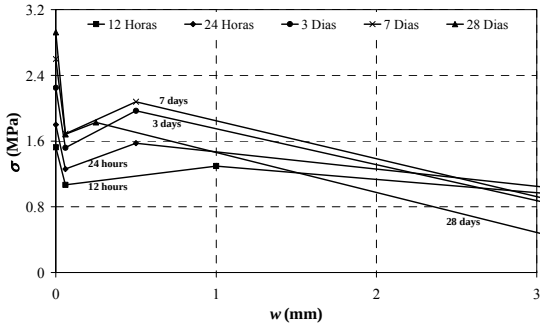

Figure 17. Influence of the SCSFRC age on the stress-crack opening diagrams.

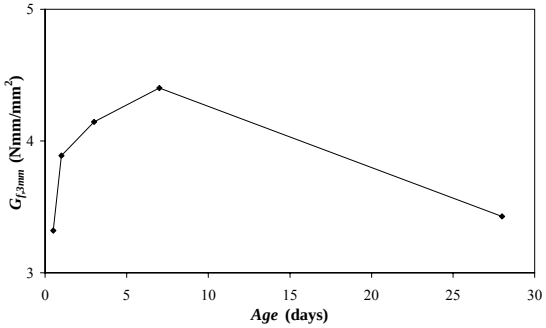

Figure 18. Influence of the SCSFRC age on the $G_{f,3mm}$.

Figure 19 shows that an high correlation exists between σ_1 and $f_{ctk,min}$, having $f_{ctk,min}$ been evaluated according to the CEB-FIP recommendations (1993).

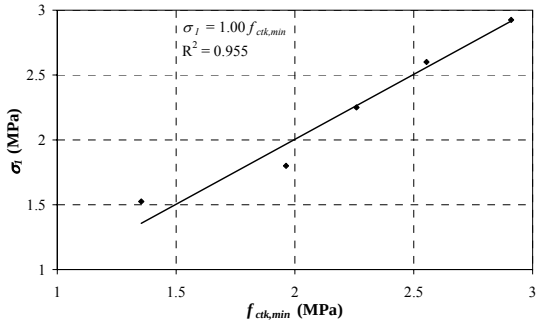

Figure 19. Relationship between σ_1 and $f_{ctk,min}$.

According to TC 162-TDF, σ_2 is linearly dependent of the $f_{eq,2}$ or $f_{R,1}$, while σ_3 is linearly dependent of the $f_{eq,3}$ or $f_{R,4}$. The σ_2 -$f_{eq,2}$, σ_2 - $f_{R,1}$ and σ_3 -$f_{eq,3}$ dependencies are confirmed in figures 20 to 22, but Figure 23 indicates that a σ_3 - $f_{R,4}$ dependence was not assured. The scalar values of the σ_2 - $f_{eq,2}$ and σ_3 - $f_{eq,3}$ dependencies are, however, distinct to those proposed by TC 162-TDF for the SFRC (0.45 and 0.37, respectively, while 0.32 and 0.40 was obtained for the SCSFRC).

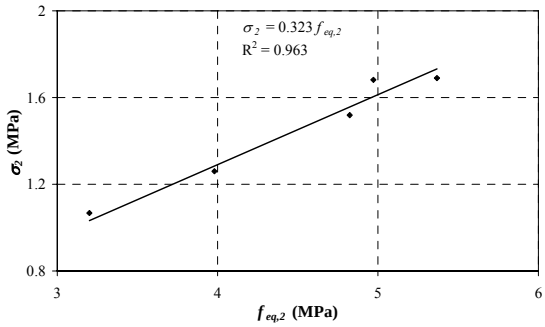

Figure 20. Relationship between σ_2 and $f_{eq,2}$.

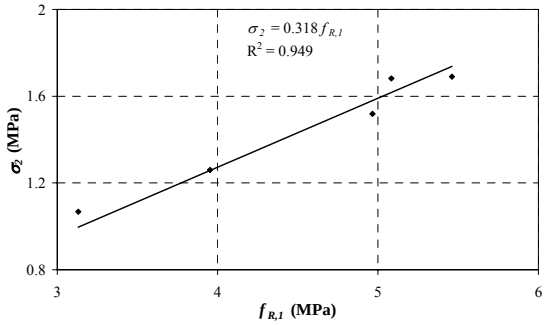

Figure 21. Relationship between σ_2 and $f_{R,1}$.

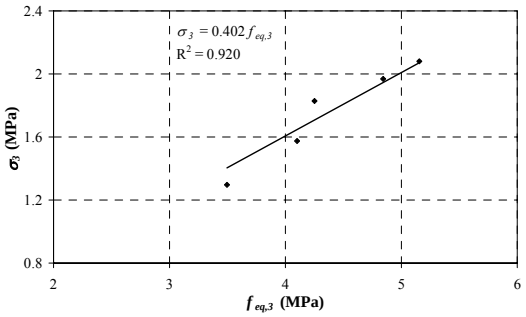

Figure 22. Relationship between σ_3 and $f_{eq,3}$.

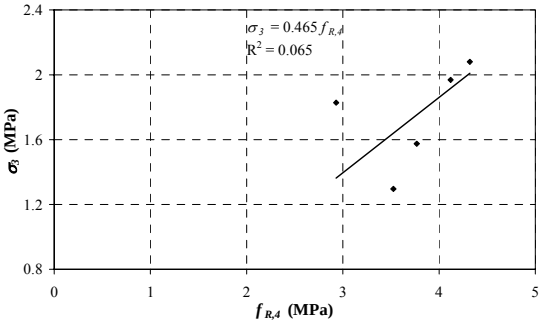

Figure 23. Relationship between σ_3 and $f_{R,4}$.

6 MODELING A SANDWICH PANEL OF SCSFRC

Figure 24 shows the cross section of a representative module of a typical sandwich SCSFRC panel to be produced by Pregaia precasting company, for the building façade applications (see also Fig. 25). To lightweight the panel, polystyrene plates of 50 mm thick are placed in the panel middle surface. The SCSFRC sandwich panel is composed by two outer layers of 30 mm thick, connected by a grid of ribs of 100 mm width. This research project involves the analysis of panels of distinct thickness for the outer layers and polystyrene plates. However, the present analysis is only restricted to the case represented in Figure 24.

Due to economical reasons and profitability of the spaces in an industrial precasting unit, the precasted panels should be demoulded and transported for stockage areas as early as possible. Therefore, lifting and transporting a panel of large dimensions, few hours after casting, is a conditioning loading case in the panel design process. Using an elasto-plastic multifixed smeared crack model implemented in the FEMIX software,

described in detail elsewhere (Sena et al. 2004a), the load factor that can be applied to the panel deadweight, to induce crack initiation at the most tensioned point(s) of the panel, was evaluated for the age of 0.5, 1, 3, 7 and 28 days. The values obtained from the experimental program and the trilinear σ-*w* diagrams obtained from inverse analysis were used to define the data required by the constitutive model. Since a smeared crack model was used, the crack opening, *w*, was converted into a crack normal strain applying a characteristic length that, in order to assure mesh objectivity (Bazant & Oh 1983), was made equal to the square root of the area of the integration point corresponding to a cracked concrete. The numerical model decomposes the strain increment vector of the load increment corresponding to the cracking initiation, in order to evaluate the precise cracking load factor. The panel was discretized by the eight-noded Serendipity finite element mesh represented in Figure 25. To simulate the crack propagation, the outer layers were discretized in three plies of 10 mm thick, and the rib in four layers of 12.5 mm. The Reissner-Mindlin theory was used to model the in-plane membrane and bending stiffness and the out-of-plane shear stiffness of the panel.

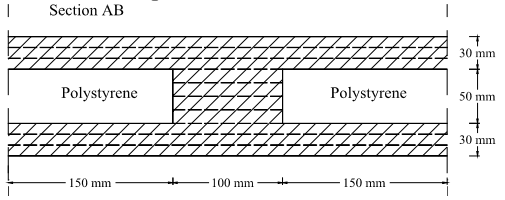

Figure 24. Representative section of the SCSFRC sandwich panel.

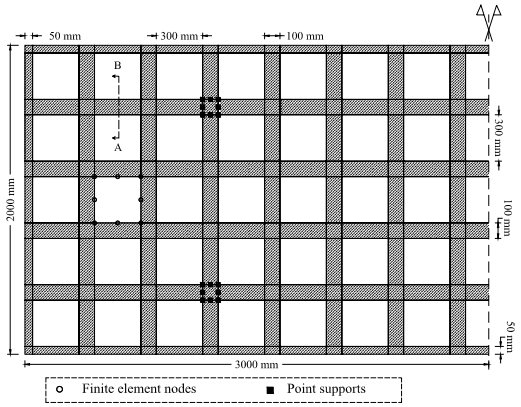

Figure 25. Finite element mesh of a half panel.

Figure 26 depicts the safety factor (*SF*) values for the SCSFRC panels of distinct ages (the multiple of the panel deadweight that induces crack initiation in the panel). At 12 hours, the safety factor is only 1.25, but increases rapidly with the SCSFRC age, getting a *SF* of 1.625 at 1 day, which is a reasonable value for this type of loading. Therefore, if this panel is hung at the locations indicated (see Fig. 25), cracking will not arise if the dynamic effects, which always occur during the lift and transportation process, do not exceed 60% of the panel deadweight.

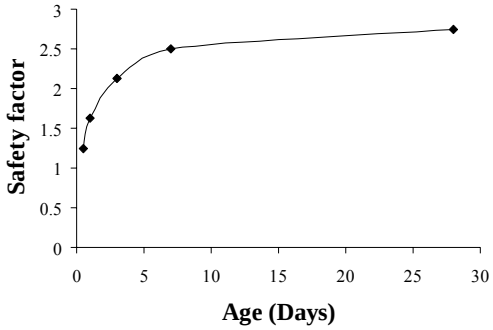

Figure 26. Safety factor for deadweight loading case, for SCSFRC panels of distinct ages.

7 CONCLUSIONS

The use of the fibre reinforced concrete (FRC) in the construction industry and the research activities involving this cement based material, in Portugal, were briefly described in the first part of the present work. In this country, the research group of Minho University is the most active in FRC domain, performing experimental and numerical research.

Selecting a research project about self-compacting steel fibre reinforced concrete (SCSFRC) for sandwich panels, carried out in consortium with Pregaia and Civitest private companies, the research strategy of this group was exemplified. The main steps of a rational method for defining a composition of high performance SCSFRC were described, since the detailed description was given in another referenced paper. An experimental program was carried out in order to assess the influence of the SCSFRC age on the bending and on the compression behaviour. For this purpose, series of notched beam bending tests and cylinder compression tests were performed at SCSFRC age of ½, 1, 3, 7 and 28 days. Taking the force-deflection relationships obtained in the

experimental bending tests, and carrying out an inverse analysis with a computational code (named FEMIX), which has constitutive models for simulating the crack propagation in a discrete or smeared approaches, a trilinear stress-crack opening diagram was obtained. This numerical strategy was appropriated to assess the influence of the age on the SCSFRC fracture parameters. The values obtained in the experimental program were taken to define the material properties of an elasto-plastic smeared crack model. Using this model, under the framework of the finite element method, the multiple of the panel deadweight that induces the cracking initiation was evaluated for the distinct analysed SCSFRC ages.

This strategy has indicated that cracking will not arise in SCSFRC panels lift up and transported from the casting to the storage areas at 24 hours, if dynamic effects occurred in this process do not surpass 60% of the panel deadweight.

8 AKNOWLEDGMENT

The study reported in this paper forms a part of the research program "Prefabricated sandwich steel fibre reinforced panels" supported by FEDER and MCT, and promoted by ADI. This project involves the University of Minho, and the Companies PREGAIA and CIVITEST. The authors wish to acknowledge the materials generously supplied by MBT (superplasticizer), SECIL (cement), Bekaert (fibres) and Comital (limestone filler).

9 REFERENCES

ASTM-C-1018. 1990. Standard test method for flexural toughness and first crack strength of fiber reinforced concrete (using beam with third-point loading (4.02). *American Society of Testing and Materials*: 637-644. Philadelphia.

ASTM-C-1550 2002. Standard test method for flexural toughness of fiber-reinforced concrete (using centrally loaded round panel). *ASTM, West Conshohocken, Pa.*.

Azevedo, A., Barros, J., Sena-Cruz, J. & Gouveia, A. 2003. Software no ensino e no projecto de estruturas (Software in structural engineering education and design). *III Portuguese-Mozambican Conference of Engineering*, *August 2003* (in Portuguese)

Balaguru, P. & Shah, S. 1992. *Fiber reinforced cement composites*. McGraw-Hill International Editions, Civil Engineering Series.

Banthia, N. & Trottier, J.F. 1995a. Test methods for flexural toughness characterization of fiber reinforced concrete: some concerns and a proposition. *ACI Materials Journal* 92(1): 48-57.

Banthia, N. & Trottier, J.F. 1995b. Concrete reinforced with deformed steel fibres, Part II: Toughness characterization. *ACI Materials Journal* 92(2): 146-154.

Barragán, B.E. 2002. *Failure and toughness of steel fiber reinforced concrete under tension and shear*. PhD Thesis, UPC, Barcelona.

Barros, J., Cunha, V., Ribeiro, A. & Antunes, J. 2004. Post-Cracking Behaviour of Steel Fibre Reinforced Concrete. Accepted to be published in the *RILEM Materials and Structures Journal*.

Bazant, Z.P. & Oh, B.H. 1983. Crack band theory for fracture of concrete. *RILEM Materials and Structures* 16(93): 155-177.

Bernard, E. 2002. Correlation in the behavior of fiber reinforced shotcrete beam and panel specimens. *RILEM Material and Structures* 35: 156-164.

CEB-FIP Model Code 1993. Comite Euro-International du Beton, Bulletin d'Information nº 213/214.

EFNARC 1996. European Federation of Producers and Applications of Specialist Products for Structures. European Specification for Sprayed concrete. *Loughborough University*.

ENV 1992-1-1. 1992. *Eurocode 2: Design of concrete structures - Part 1: General rules and rules for buildings*. Technical report, European pre-standard.

Gopalaratnam, V.S. *et al*. 1991. Fracture toughness of fiber reinforced concrete. *ACI Materials Journal* 88(4): 339-353.

Japan Society of Civil Engineers. 1984. Method of test for flexural strength and flexural toughness of fiber reinforced concrete. *Standard SF-4*: 58-66.

Pereira, E., Barros, J., Ribeiro, A. & Camões, A. 2004. Post-cracking behaviour of self-compacting steel fibre reinforced concrete. Accepted to be published in the *BEFIB; Proc. Intern. Symp.,Varenna, Italy, 20-22 September*.

RILEM Draft Recommendation, 50-FMC Committee Fracture Mechanics of Concrete 1985. Determination of the fracture energy of mortar and concrete by means of three-point bending tests on notched beams. *Materials and Structures* 85(85): 285-290.

Schellekens, J. 1990. Interface elements in finite element analysis. *TU-Delft report 25.2-90-5-17/TNO-IBBC,* report BI-90-165.

Sena, J., Barros, J. & Azevedo, A. 2004b. Elasto-plastic multi-fixed smeared crack model for concrete. Relatório técnico 04-DEC/E-05, *Dep. of Civil Eng., University of Minho*.

Sena, J., Barros, J., Fernandes, A., Azevedo, A. & Camões, A. 2004a. Stress-crack opening relationship of enhanced performance concrete. *9th Portuguese Conference on Fracture*, *Setúbal, Portugal, 18-20 February 2004*.

Noghabai, K. 1998. Effect of tension softening on the performance of concrete computational studis. PhD Thesis, Dept. of Civil and Mining Eng., Division of Structural Eng., Lülea University of Technology, Sweden.

Vandewalle, L. *et al.* 2000a. Test and design methods for steel fiber reinforced concrete. Recommendations for bending test. *Materials and Structures* 33(225): 3-5.

Untiveros, C. M. A. 2002. Estudio experimental del comportamiento del hormigón confinado sometido a compresión, PhD Thesis, UPC, Barcelona.

Vandewalle, L. *et al.* 2000b. Test and design methods for steel fiber reinforced concrete. Recommendations for σ-ε design method. *Materials and Structures* 33(226): 75-81.

Vandewalle, L. *et al.* 2002. Test and design methods for steel fibre reinforced concrete - Final Recommendation. *Materials and Structures* 35(253): 579-582.

Vandewalle, L. *et al.* 2003. Test and design methods for steel fibre reinforced concrete – σ-ε design method - Final Recommendation. *Materials and Structures* 36(262): 560-567.